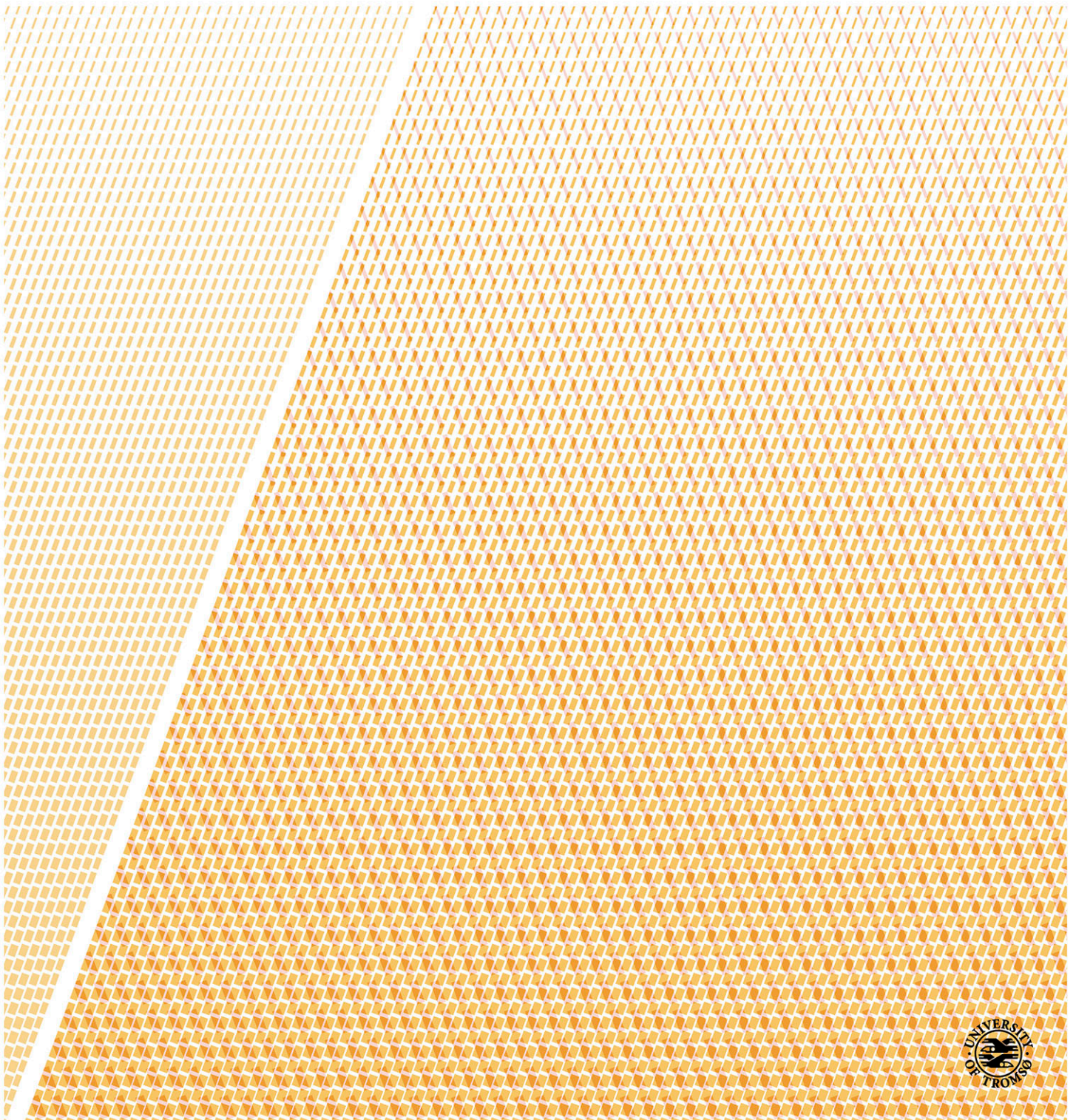# Past and present natural methane seepage on the northern Norwegian continental shelf

—

Simone Sauer
A dissertation for the degree of Philosophiae Doctor – April 2016

<u>Dissertation for the degree of Philosophiae Doctor</u>

Past and present natural methane seepage on the northern Norwegian continental shelf

Simone Sauer

Department of Geology

Faculty of Science and Technology

University of Tromsø

The Arctic University of Norway

April 2016

Dedicated to my grandparents Franz and Klara Sauer

Preface

This doctoral thesis was carried out from November 2012 to April 2016 at the Geological Survey of Norway, while I was enrolled as a PhD candidate at the Arctic University of Norway, Tromsø. I received supervision from Jochen Knies (NGU), Aivo Lepland (NGU), Carsten Schubert (EAWAG) and Jürgen Mienert (UiT). Funding sources were RWE Dea (now DEA Norge AS) (C-1648/1) and the Norwegian Research Council through CAGE-Centre for Arctic Gas Hydrate, Environment and Climate (grant 223259).

Acknowledgments

Table of contents

1   List of papers

Paper I

Sauer, S., Knies, J., Lepland, A., Chand, S., Eichinger, F., Schubert, C.J., 2015. **Hydrocarbon sources of cold seeps off the Vesterålen coast, northern Norway**. Chemical Geology, 417: 371-382.

Paper II

Sauer, S., Hong, W.-L., Knies, J., Lepland, A., Forwick, M., Klug, M., Eichinger, F., Baranwal, S., Crémière, A., Chand, S., Schubert, C.J., **Isotopic insights into the sources and turnover of organic carbon and methane in fjord and shelf sediments off northern Norway**. Accepted at G-cubed with moderate revision

Paper III

Sauer, S., Crémière, A., Knies, J., Lepland, A., Sahy, D., Martma, T., Noble, S.R., Schönenberger, J., Klug, M., Schubert, C.J., **Methane-derived authigenic carbonates from the Hola trough seep area, Northern Norway: formation controls and chronology**. To be submitted to Arktos.

2   Introduction and motivation

The two most important reasons for studying methane in the Earth system are (1) its significance as a potential energy source from methane hydrate reservoirs and (2) its strong effect as a greenhouse gas in the Earth's atmosphere (Lashof and Ahuja, 1990; Makogon et al., 2007). From an energy source point of view, it is estimated that actually 53% of all fossil fuel, including coal, oil and natural gas, is stored in the form of methane hydrate in the sub seabed and beneath arctic permafrost (Lee and Holder, 2001). The gas hydrates are not only relevant as an energy source but also represent a potential large pool of methane that could be released to the oceans and atmosphere in the light of future climate predictions. One molecule of methane has a 'greenhouse' effect that is 25 times stronger than the effect of one carbon dioxide molecule in the atmosphere (Lelieveld et al., 1998). Furthermore, methane has an effect not only as a greenhouse gas, but its atmospheric chemistry adds to the radiative forcing as well (Dlugokencky et al., 2011) and thus it plays an important role considering future global climate change (IPCC 2013). The present methane concentration in the atmosphere is 1.84 ppm (http://www.esrl.noaa.gov/gmd/ccgg/) whereas the pre-industrial value was 0.7 ppm (Etheridge et al., 1998) and the concentration was only 0.35 ppm during the last glacial period (Kvenvolden and Rogers, 2005). Methane has a short lifetime of approximately 8 years in the atmosphere (Lelieveld et al., 1998). The contribution of methane in the atmosphere to the current global warming is estimated to be around 15% (Badr et al., 1991), hence in order to improve climate predictions it is crucial to understand and constrain sources and sinks of atmospheric methane. Methane sources to the atmosphere are divided into natural and anthropogenic sources, and further into terrestrial and aquatic sources (Table 1). The major sink of atmospheric methane is through the oxidation by hydroxyl radicals in the troposphere, accounting for around 90%. Other sinks are stratospheric reactions and microbial oxidation in soils (Lelieveld et al., 1998; Kirschke et al., 2013 and references therein). Although most of the sources and sinks of atmospheric methane have been identified, their relative contributions are still uncertain, and one of the major unknowns is the

emission of methane from oceans (Kirschke et al., 2013). Thus, it is important to study the behaviour and fate of methane in the marine environment to ultimately understand the processes that enhance or inhibit its release from the seafloor to the oceans and ultimately to the atmosphere.

Table 1: Atmospheric methane sources (Kvenvolden and Rogers, 2005; Kirschke et al., 2013).

Natural atmospheric methane sources	Anthropogenic atmospheric methane sources
• Wetlands • Fresh water • Termites • Wildfires • Terrestrial seeps • Marine seeps • Mud volcanoes (marine and terrestrial) • Termites • permafrost	• Fossil fuel burning (coal oil natural gas) • Freshwater reservoirs (dams) • Domestic ruminants • Organic waste deposits • Rice agriculture • Biomass burning

Furthermore, regarding past climate variations, the thermal dissociation of gas hydrates on continental shelves, followed by the release of methane from the seafloor, has been suggested as one reason for the negative δ^{13}C isotope excursion during the Paleocene-Eocene-Thermal-Maximum and other hyperthermal events (Kennett et al., 2000; Dickens, 2011 and references therein). A positive warming feedback by the gas hydrate dissociation is suggested due to oxidation to CO_2 in the oceans and atmosphere. However, this theory still lacks proof. To improve the understanding of the relationship between methane-related processes and past climate variations it is important to better constrain past methane escape episodes by for example dating of methane-derived authigenic carbonates.

Thus, my PhD thesis represents a holistic approach of studying the physical, chemical and biological processes related to methane cycling in the marine environment. It deals with processes that affect methane cycling at present and in the past and which take place below the surface of the oceans; in the water column, on the seafloor and within the sediments (Figure 1).
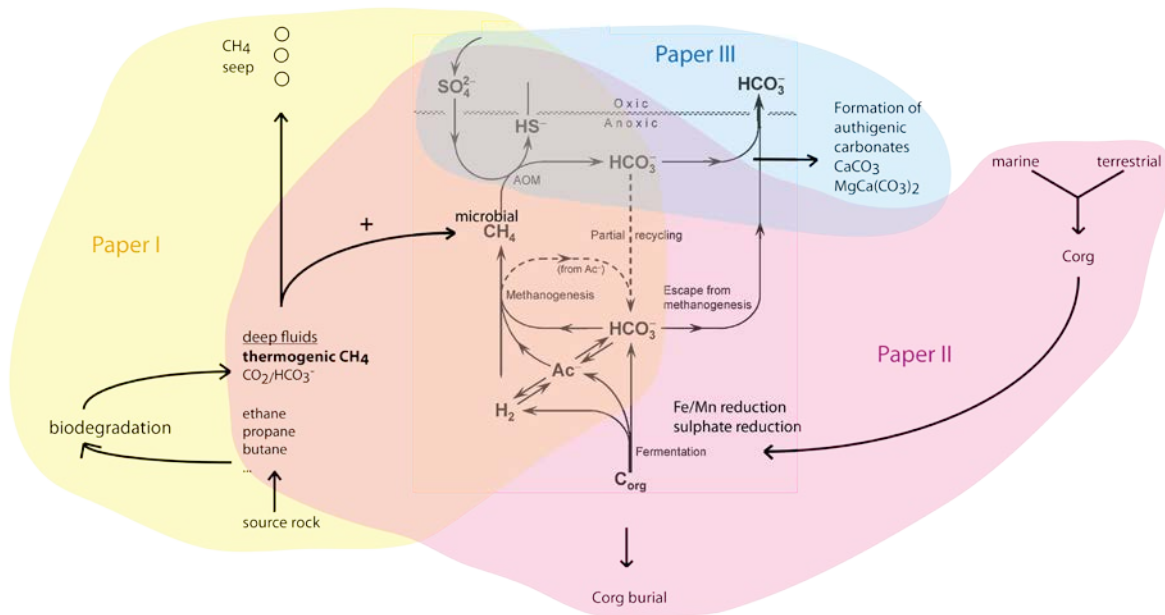
Figure 1: Schematic of the marine methane cycle covered by the three articles included in this PhD thesis (modified from Holler et al. (2009)).

Paper I deals with current state of the hydrocarbon system on the continental shelf offshore the Vesterålen Islands; an area where active methane seepage had been identified before, but which represents a fairly little investigated part of the Norwegian shelf compared to the main petroleum provinces in the Norwegian and Barents Sea. The aspects covered in Paper I are outlined in the left part of Figure 1 and include the investigation of methane and C_2-C_4 hydrocarbons, a possible source rock, migration pathway to the seafloor, biogeochemical processes in the methane-charged sediments and the nature of methane flux in the upper sedimentary column and where it enters the water column. We used hydroacoustic methods, single and multibeam echosounder, and CTD water column sampling to detect gas flares and confirm the escape of methane from the seafloor to the water column. Pore water data helped to assess the spatial heterogeneity of methane flux to the sediment surface and where it was potentially consumed in the sediment by anaerobic oxidation. Isotope analyses of methane sampled from the sediment assisted in determining whether the dominant methane source was thermogenic or microbial, and C_2 to C_4 hydrocarbon isotope analyses provided insight into processes of biodegradation affecting the petroleum reservoir. 2D seismic profiles, supplemented with well data from the literature, lead to the identification of a possible

source rock and migration along a major unconformity between the underlying basement and the Mesozoic sedimentary rocks.

Paper II evaluates the carbon cycle in the surface sediments of the Vesterålen shelf seep site with the aid of a comparison site with a distinctly different carbon source and sedimentation regime in a northern Norwegian fjord. The processes considered in Paper II are mainly the aspects on the right site of Figure 1, including organic matter sedimentation, degradation, and transformation to methane. Sedimentological investigations and radiocarbon dating were used to establish approximate sedimentation rates, and combined with organic carbon content resulted in estimates of organic matter burial at each site. Chemical and isotope composition of the organic matter helped to differentiate between marine and terrestrial organic matter sources. Organic matter source and burial showed to have a substantial influence on early diagenetic reactions in the sediments resulting in notably different estimates of sulphate reduction and methanogenesis based on pore water modelling. These results were directly linked to the interpretation of gas source in the sediments and showed that the seep site was mainly influenced by carbon input via the rise of thermogenic methane rich-fluids. In contrast, the fjord site is completely dominated by marine organic matter deposition originating from primary production in the water column resulting in microbial methane production in the sediments.

Paper III adds temporal constraints on the methane seepage on the Vesterålen shelf. We investigated authigenic carbonate crusts and nodules which formed due to high rates of anaerobic oxidation of methane (Figure 1) in different sediment depths and are partly exposed at the seafloor now due to erosion. Sampling sites were chosen based on a high resolution synthetic aperture sonar survey clearly showing several fields of carbonate crusts in the study area. Isotope investigations of these seep carbonates revealed the carbon and oxygen sources for their formation and different carbonate mineralogy further shed light on formation environments. U-Th dating results of two

crusts from our sampling campaign and one from a previous study show clustering of ages within the

Holocene and a tentative correlation with high seismicity periods.

3   Study area

3.1   Northern Norwegian shelf and fjord

All samples that were used in this thesis and the coordinates of sample locations are summarized in Figure 2. The main study area (Paper I and III) is the Hola trough on the shelf offshore the Vesterålen islands. Paper II uses both data from the Hola trough and from one sample in Ullsfjorden for comparison (Figure 2).

Region	Station name	Latitiude	Longitude
Hola trough	HH13-GC24	68.9174	14.2851
	HH13-GC51	68.9179	14.2858
	HH13-GC52	68.9178	14.2860
	CTD 209	68.9178	14.2839
	MDAC 2	68.9183	14.2836
	MDAC 5	68.9170	14.2847
Ullsfjorden	HH13-GC36	69.7852	19.8096
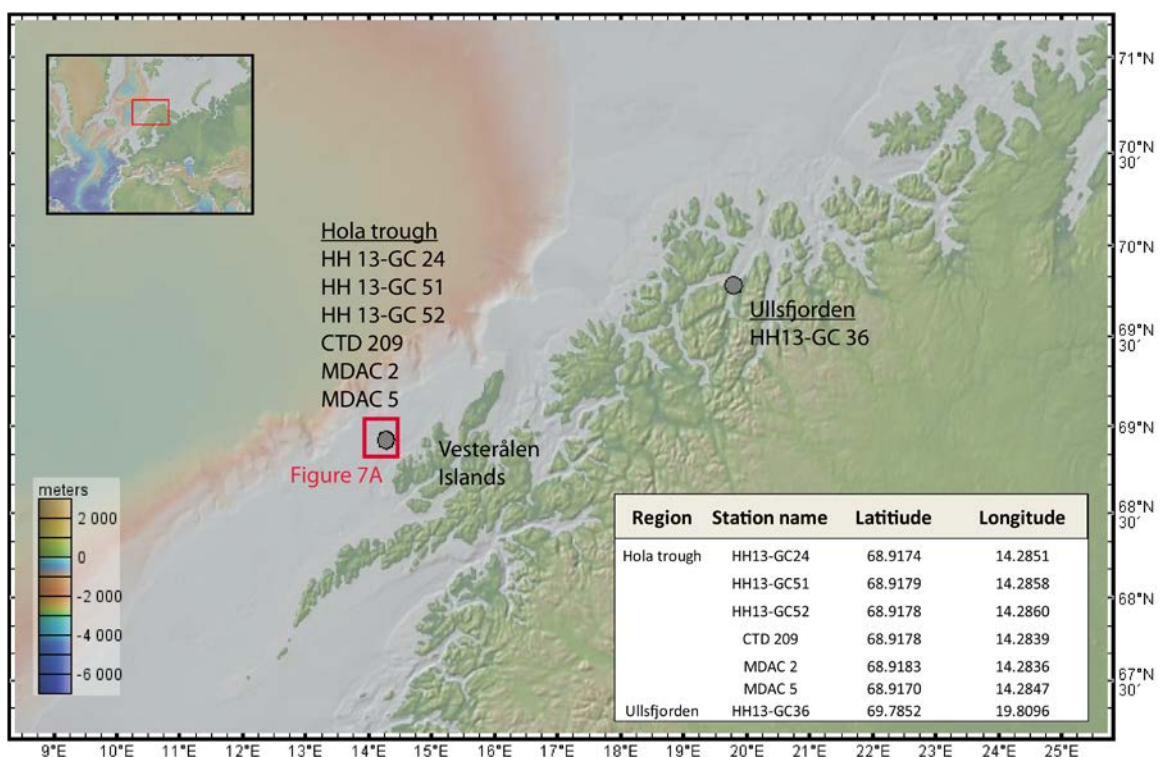
Figure 2: The northern Norwegian shelf with the main study area and sample locations in the Hola trough and one comparison station in Ullsfjorden (Map produced with Geomapapp).

Hola trough

The continental shelf offshore the Vesterålen Islands (Figure 2), northern Norway, is relatively narrow and characterized by numerous banks separated by over-deepened cross-shelf troughs which were formed during the last glaciations (Bøe et al., 2009; Godø et al., 2012). The Hola trough is ca. 12 km wide with water depths reaching 270 m at the deepest point and confined by the banks Vesterålsgrunnen to the NE (Figure 3A) and Eggagrunnen to the SW. The NE flank is sloping at 4° and

the SW flank at less than 2° (Godø et al., 2012). Notable geomorphological features are several sand wave fields and cold water coral mounds (Figure 3), inhabited by the cold water coral *Lophelia pertusa* (Thorsnes et al., 2015). Active seepage and gas flares were first reported from the Hola trough by Chand et al. (2008) (Figure 3B).

Figure 3: (A) Shaded relief of one part of the Hola trough showing the NE flank in the upper right corner. Cold water coral reefs are highlighted with green circles and sandwave fields with red. The black arrow shows the location and direction of view in (B). (B) 3D view of the Hola trough with gas flares and coral mounds (5 x vertical exaggeration) (from Thorsnes et al. (2015))
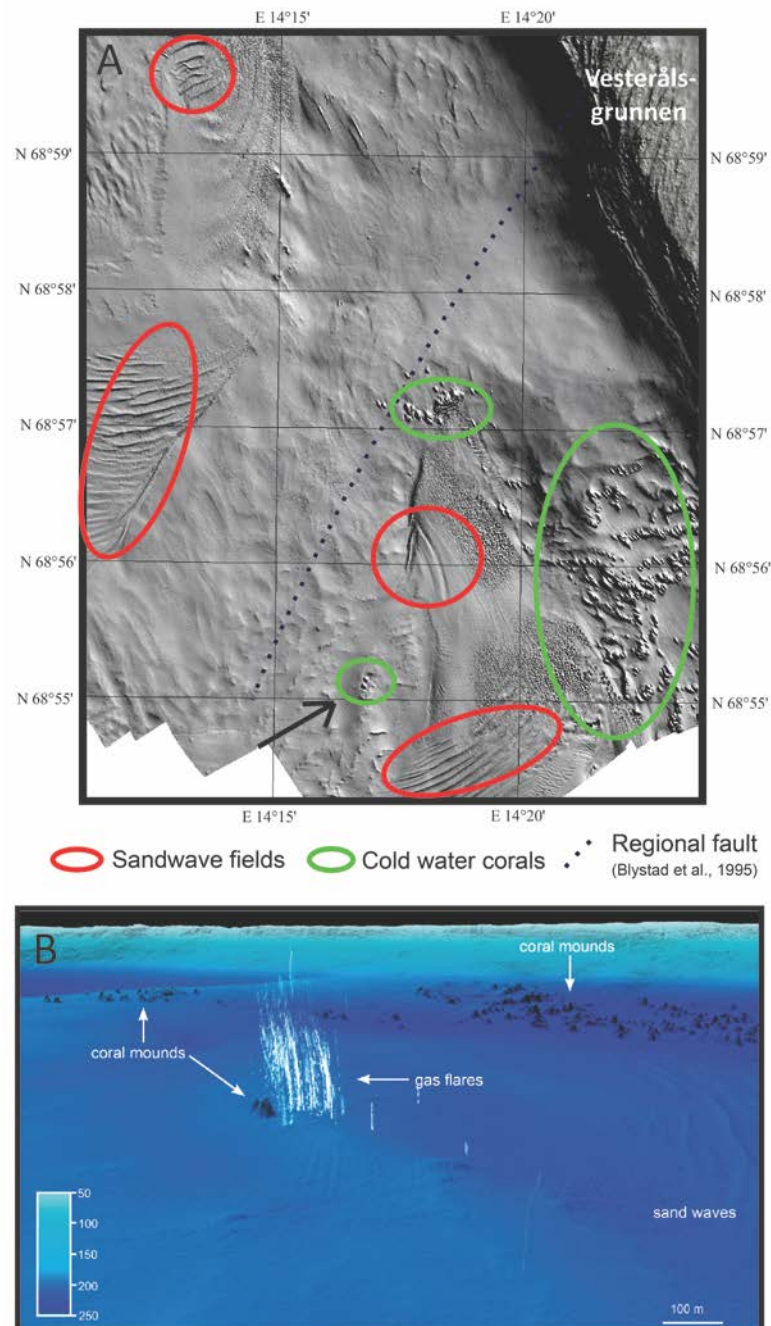
Ullsfjorden

Ullsfjorden is a north-south oriented fjord in Troms County, northern Norway (Figure 2). The fjord is ca. 70 km long with a maximum water depth of 285 m (Plassen and Vorren, 2003b). The sediment infill is largely composed of glaciomarine sediments with thicknesses up to 200 m deposited during deglaciation (Vorren et al., 1989). Ullsfjorden was deglaciated between ca. 15-11 cal ka BP and sediment deposition in an open marine environment started around 11 cal ka BP (Plassen and Vorren, 2003a). The bottom of Ullsfjorden is characterized by ubiquitous pockmarks (Plassen and Vorren, 2003b), suggested to have been formed as a result of gas escape or groundwater-related processes (Hovland and Judd, 1988; Plassen and Vorren, 2003b).

3.2   Oceanography of the northern Norwegian margin

Offshore the Vesterålen Islands the Norwegian Coastal Current (NCC) and the Norwegian Atlantic Current (NWAC) are the dominant water masses (Figure 4). The NCC flows along the coast coming from the southwest and transports Norwegian Coastal Water (NCW), whereas the NWAC follows the continental slope, coming from the southwest, transporting warm and saline Atlantic Water (AW) (Figure 4B), and splitting into one branch towards Spitsbergen and one branch going eastward into the Barents Sea (Figure 4A). The annual mean bottom water temperature is around 7°C on the shelf, but decreases fast down the slope (Albretsen et al., 2011).

Since deglaciation winnowing along the shelf and upper slope by the Norwegian Atlantic current is the dominant sedimentary process (Vorren et al., 1984; Laberg et al., 2005; Bellec et al., 2012). Present estimates of bottom current velocities are up to 0.7 m s^{-1} (Bøe et al., 2009) which created a coarse grained lag deposit as the very top layer in the Hola trough. Such erosional regime has probably been active since the beginning of the Holocene when the full intrusion of the Norwegian Atlantic current was established (e.g. Vorren et al., 1984).
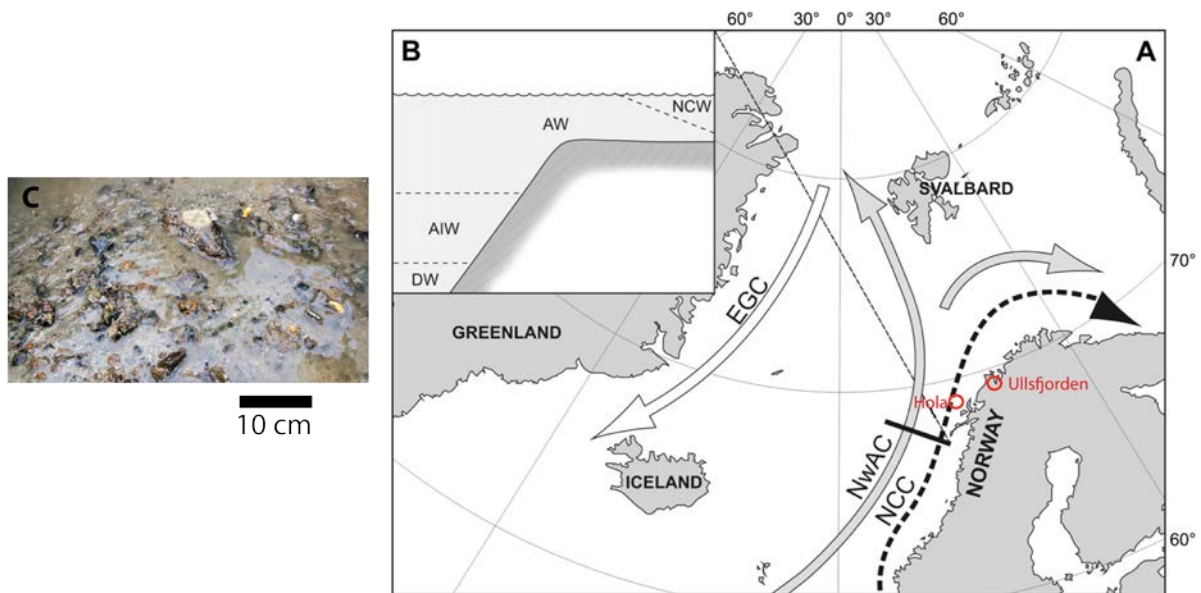
Figure 4: (A) Illustration of simplified oceanographic surface currents on the shelf and slope, with (B) a cross section just south of the Lofoten Islands (from Rørvik et al. (2010)). The red circles indicate the study areas in the Hola trough and Ullsfjord. (C) Coarse surface sediment sampled from the Hola trough using a box core; the lag deposit results from strong winnowing by the Norwegian Atlantic current.

3.3 Geology of the Norwegian continental margin

The continental shelf and slope along the Norwegian continental margin vary considerably in width and steepness. This structure formed in response to the opening of the Norwegian-Greenland Sea. (Faleide et al., 2008) (Figure 5A). The Norwegian margin has experienced several rift episodes and the last one, during the late Cretaceous to Paleocene, was followed by continental break up at the end of the Paloecene-Eocene transition (Byrkjeland 2000), around 55 Ma ago, accompanied by intense magmatic activity on the mid-Norwegian margin (Faleide et al., 2008). The Lofoten-Vesterålen margin is characterised by a narrow shelf and a steep slope (Figure 5A) and the Moho depth in coastal areas is ca. 30 km (Tsikalas et al., 2005).
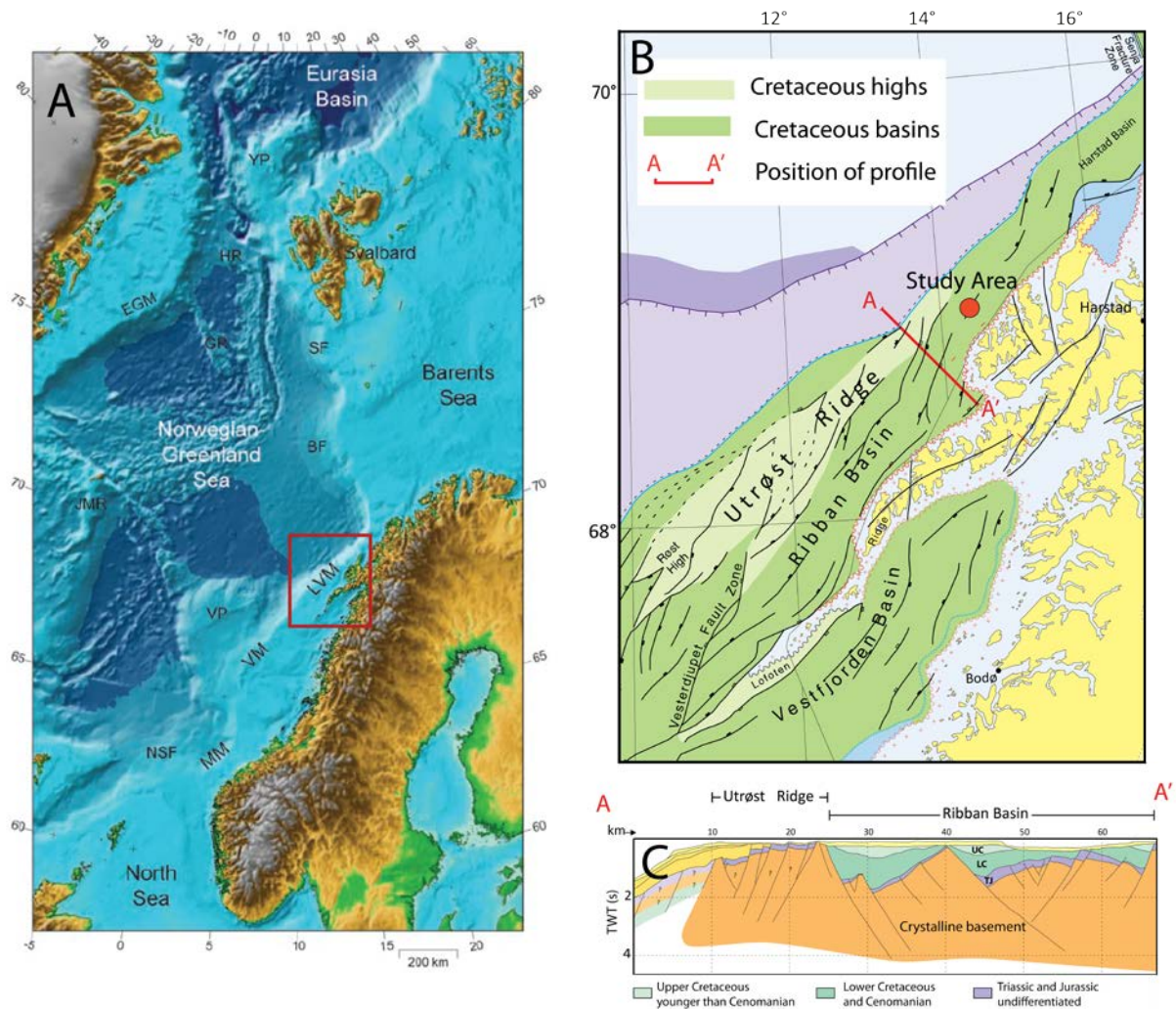
Figure 5: (A) Regional setting of the Norwegian continental margin (LVM = Lofoten Vesterålen margin, (Faleide et al., 2008)), (B) The geological structures of the Lofoten Vesterålen margin, indicating the location of the study area (red dot) and a cross section (red line). (C) Cross section of the continental shelf just south of the Vesterålen Islands showing asymmetric half-graben structures and Cretaceous basins (modified from Blystad et al. (1995)).

The Cretaceous sedimentary basins on this part of the shelf form asymmetric half-graben structures (Figure 5C) and are bounded dominantly by extensional faults (Bergh et al., 2007). The Lofoten-Vesterålen margin is underlain by Precambrian crystalline basement, followed by Lower-Middle Jurassic sandstones with coal rich layers, Upper Jurassic sandy and calcareous mudstones and Lower-Upper Cretaceous claystones, siltstones and sandstones with organic rich intervals (Henningsen and Tveten, 1998). The Quaternary sediments covering the bedrock were deposited during several glacial cycles (e.g. Ottesen et al., 2002). Since the late Pliocene (ca. 3 Ma) the tectonic uplift of Fennoscandia and the Northern Hemisphere glaciations have resulted in greatly increased sedimentation rates on

the Norwegian margin and rapid progradation (Byrkjeland et al., 2000) due to ice sheets which have

reached the shelf break repeatedly delivering large amounts of sediments to the shelf environment

(Dowdeswell et al., 1996; Laberg et al., 2005). This formed regional large depocenters near the shelf

edge for example offshore Mid-Norway, and smaller depocenters, for example offshore Nordland

(Ottesen et al., 2002; Eidvin et al., 2014). In fact, more than 50% of the Cenozoic sediment volume on

the Norwegian margin has been deposited during the last 2.6 Ma (Byrkjeland et al., 2000). The

enhanced sediment supply created numerous trough mouth fans (Rydningen et al., 2015), and

unstable conditions along the shelf edge which also led to several Holocene slides along the

continental slope (Figures 6A) (Laberg and Vorren, 2000; Laberg et al., 2000; Haflidason et al., 2005).

The deglaciation of the Vesterålen shelf is outlined in Figure 6B and took place mainly between 22-16

cal ka BP (Vorren et al., 2015), with several episodes of waxing and waning of the ice sheet and the

creation of grounding zone wedges caused by still-stands of the ice sheet during retreat (Batchelor
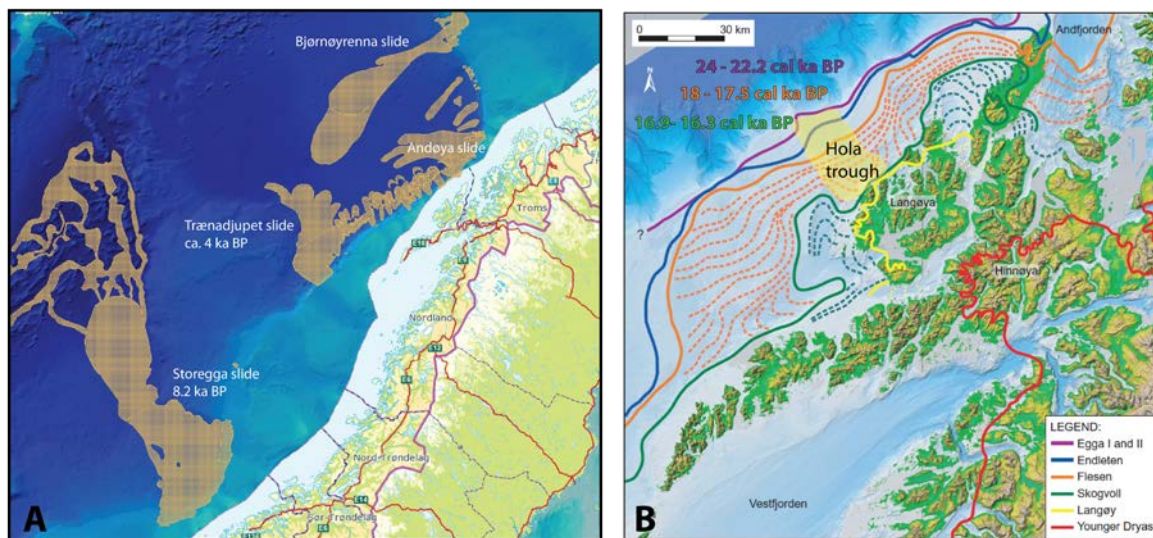
and Dowdeswell, 2015).

Figure 6: (A) Deglaciation of the Vesterålen-Lofoten shelf area (modified from Vorren et al. (2015)), showing that the ice sheet had probably retreated from the Hola trough at ca. 16 cal ka BP. (B) Major submarine slides on the northern Norwegian margin (Mareano.no)
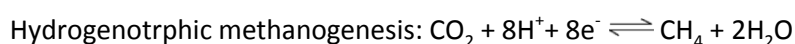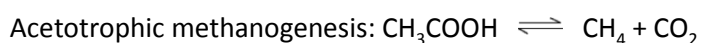
4   Background

4.1   Methane sources in the marine environment

Methane can be formed by three principle processes, two of which involve the transformation of organic matter and one that is abiotic (abiogenic). The two processes involving organic matter are the microbially mediated methane formation and the geologically controlled thermogenic methane formation in sedimentary rocks. The essential prerequisite for both processes is the abundance of at least 0.5% organic matter in the sediment (Judd, 2004), mostly lipids and carbohydrates from marine and terrestrial organic matter (Etiope and Schoell, 2014).

4.1.1   Microbial methane

The microbial, also called biogenic, formation of methane is mediated by methanogenic archaea (Kvenvolden and Rogers, 2005) in shallow sediments. Microbial methanogenesis is the last step in the remineralisations of organic matter (Froelich et al., 1979) and generally starts beneath the sulphate reduction zone. Typically, the generation of microbial methane gas takes place within fine-grained sediments with a high initial content of organic matter (Judd, 2000). The temperature range for microbial methanogenesis is relatively wide with an optimum for methanogenic archaea between 35 and 45°C and a maximum at about 60°C (Rice, 1992). This means microbial methanogenesis can commonly occur until a depth of about 2 km, assuming an average geothermal gradient. The two main methanogenic pathways are acetotrophic (1) and hydrogenotrophic (2) methanogenesis, also referred to as acetate fermentation and carbonate reduction, respectively (Whiticar, 1999). The reactions are as follows:

Acetotrophic methanogenesis: $CH_3COOH \rightleftharpoons CH_4 + CO_2$

Hydrogenotrphic methanogenesis: $CO_2 + 8H^+ + 8e^- \rightleftharpoons CH_4 + 2H_2O$

Whiticar (1999) suggests that hydrogenotrophic methanogenesis is the dominant process in the marine environment because sulphate reducing bacteria use acetate as a substrate which makes it less available to acetate fermenting microbes.

4.1.2   Thermogenic methane

Thermogenic formation of methane, which takes place by the thermocatalytic breakdown of complex organic molecules called kerogen, is part of the petroleum generating process. Land-derived organic matter generally generates gas and liquids whereas marine algal organic matter rather produces liquids. This thermal conversion of organic matter occurs deep within sedimentary basins (Judd, 2004) usually at subbottom depths exceeding 1000 m (Floodgate and Judd, 1992). Methane formation can continue to sediment depths of 4 or 5 km and takes place at temperatures above 80 °C, but is only the dominant process in the last stage of thermogenic hydrocarbon production at temperatures above 150 °C (e.g. Clayton, 1991). After generation from the source rock, methane may migrate towards the seabed by bulk flow of bubbles driven by buoyancy, by diffusion or in solution in pore waters (Judd, 2000). However, proportions of the generated methane can be trapped in petroleum reservoirs during ascent.

4.1.3   Abiotic methane

Abiotic or abiogenic methane production is another, but poorly understood, category of methane formation. Abiotic methane is generated by (1) magmatic and (2) gas-water-rock reactions that do not directly involve organic matter (Etiope and Schoell, 2014). Most of the abiotic gas found on Earth is produced by low temperature gas-water-rock reactions (Etiope and Sherwood Lollar, 2013).

Different inorganic reactions producing methane are known, including Fischer-Tropsch type reactions, which are the most widely suggested mechanism for creating large quantities of abiotic methane, where methane is formed from CO_2 or CO with H_2 involving metal catalysts.

The serpentinization reaction occurring in the vicinity of slow- to ultraslow spreading centres/mid ocean ridges at temperatures above 300°C is another process producing abiotic methane (Reeburgh, 2007; Cannat et al., 2010). The serpentinization reaction produces hydrogen which reacts with carbon dioxide to form methane:

$$CO_2 + 4H_2 \rightleftharpoons CH_4 + 2H_2O$$
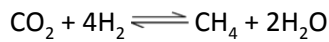
It is not questioned any longer whether or not abiotic methane can be formed in natural environments, however the question of possible commercial quantities of abiotic natural gas is still debated (Glasby, 2006). A recent study by (Johnson et al., 2015) suggests that abiotic methane could actually be the dominant source of gas in a gas-charged sediment drift close to an ultra-slow spreading centre in the eastern Fram Strait, the Atlantic-Arctic gateway. However, there has yet been no confirmation of this hypothesis by the sampling and isotopic analysis of this gas.

4.2   Methane sinks in the marine environment

4.2.1   Anaerobic oxidation of methane (AOM)

Within the sediments microbial communities performing anaerobic oxidation of methane (AOM) form a very effective methane sink (e.g. Sommer et al., 2006). AOM is estimated to remove > 80% of sedimentary methane before it can reach the water column (Hinrichs and Boetius, 2003; Reeburgh, 2007). This anaerobic oxidation of methane was first revealed in anoxic marine sediments in the 1970s (e.g. Reeburgh, 1976). The net reaction of anaerobic methane oxidation is

$$CH_4 + SO_4^{2-} \rightarrow HCO_3^- + HS^- + H_2O.$$

This reaction is performed by a consortium of sulphate reducing bacteria and methane oxidising archaea (Hinrichs et al., 1999; Boetius et al., 2000; Orphan et al., 2001). At least two phylogenetically distinct groups of archaea, ANME-1 and ANME-2, can perform AOM (Valentine, 2002). The sedimentary zone of AOM is called the sulphate-methane-transition (SMT) which shows both the depletion in pore water sulphate and pore water methane concentrations and is observed both in diffusion- as well as advection-dominated environments. This biogeochemical reaction zone has been observed in many marine sediments along continental margins (Valentine, 2002). It and can vary in depth between a few centimetres above methane hydrate deposits and in methane seep settings

(e.g. Fischer et al., 2012) down to sediment depths of more than 100 m (D'Hondt et al., 2002). After the discovery of sulphate-dependent AOM, other electron acceptors have been reported that can facilitate AOM as well, such as nitrite and nitrate (e.g. Raghoebarsing et al., 2006; Ettwig et al., 2008) or iron and manganese oxides (e.g. Beal et al., 2009; Rooze et al., 2016).

4.2.2   Aerobic oxidation of methane (MOx)

The seep-derived methane, which is not consumed by AOM in the sediment but enters the water column, can be oxidised within the water column by aerobic methane oxidation (MOx), preventing it from reaching the atmosphere (Reeburgh, 2007):

$$CH_4 + 2O_2 \rightarrow CO_2 + H_2O$$
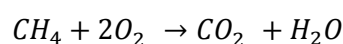
However, so far there have been relatively few measurements of methane oxidation rates in the ocean (using tracers like ^{14}C-CH$_4$, ^{3}H-CH$_4$ and CFC-11), hence the understanding is still poor (Reeburgh, 2007). In general, oxidation rates are probably influenced by temperature, pressure and methane concentration (Scranton and Brewer, 1978). Furthermore, a recent study by Steinle et al. (2015) shows the relationship of water mass properties and methanotrophic activity at methane seeps which is subject to rapid changes due to meandering currents offshore western Svalbard. This is explained by varying compositions of the methanotrophic community in the different water masses.

Over half of the total methane produced on Earth is estimated to be consumed by microbial aerobic and anaerobic methane oxidation (Kvenvolden and Rogers, 2005).

4.3   Methane storage in gas hydrates

Gas hydrate, a crystalline substance composed of a cage of water molecules that host gas molecules such as methane, is an intermediate storage system for sedimentary methane. Due to its metastable and dynamic characteristics, it can act as both source and sink of methane over geologic time (Kvenvolden and Rogers, 2005). During the current state of global change methane hydrate

dissociation is discussed as potential positive feedback, provided that it is emitted to the atmosphere. At present there are supposedly large reservoirs of gas hydrate along continental margins, but estimates vary significantly between 170-12700 Gt C stored in gas hydrates (Dickens, 2011 and references therein), showing the huge uncertainties in the current gas hydrate reservoir estimates.

Especially in Arctic regions where warming rates are highest (Bekryaev et al., 2010), it is important to investigate if the anthropogenic warming leads to increased rates of gas hydrate dissociation and if the released methane enters the atmosphere. There is no consensus yet, but model-based estimates suggest that methane released below 200 m is almost entirely consumed before reaching the sea surface (McGinnis et al., 2006). Only at shallow marine seep sites there are indications for the transport of methane all the way to the atmosphere (Shakhova et al., 2010).

4.4 Seeps

The methane produced microbially, thermogenically or abiotically, and which has bypassed potential petroleum traps, avoided being incorporated into gas hydrate or being consumed by the benthic methane filter can enter the ocean in different ways; most commonly by methane seepage from the seafloor. Seeps are formed in places where the rate of methane production and/or migration exceeds the rate of utilisation and so there is a flux from the sediment into the water column. The seeps can be divided into different categories: micro seeps (diffusion controlled), macro seeps and mud volcanoes (advection controlled) (Figure 7, Reeburgh (2007)). The term micro seep is used for the slow, continuous seepage of hydrocarbon gases like methane. The depth of the methane origin is generally rather shallow for diffusion controlled seeps in contrast to deeper methane sources in the case of macro seeps and mud volcanoes. These deeper sources can be either leaking petroleum reservoirs or the dissociation of gas hydrate.
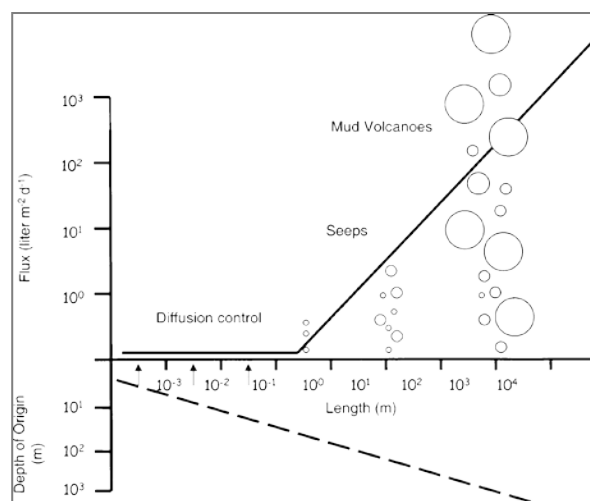
Figure 7: Length, depth and flux scales of methane addition to the ocean from a range of sources (from Reeburgh (2007))

Seeps occur in a wide range of oceanographic settings such as coastal areas, continental shelves, slopes, rises and the abyssal plains. Moreover, the geological context can vary between, convergent, divergent, transform plate boundaries and intraplate boundaries (Judd and Hovland, 2007).

4.5   Information contained in methane and higher hydrocarbon isotope composition

4.5.1   Methane formation

Kinetic isotope effects during methane production and methane oxidation change the isotopic composition of methane and provide a means for identifying the formation and subsequent processes involving methane (Judd and Hovland, 2007). The three different sources of methane (microbial, thermogenic, abiotic) may be distinguished by their stable carbon and hydrogen isotopic signature and, furthermore, by the relative proportion of other higher hydrocarbons that are present as well (Whiticar, 2000). Microbial methane generally has carbon isotope values $\delta^{13}C < -50‰$ with values ranging as low as -110‰ (Figure 8). This is caused by large isotope fractionation during methanogenesis. The isotopic composition of microbial methane is determined by the isotope signature of the precursor material (dissolved inorganic carbon or acetate) and by the kinetic isotope effect, which means molecules with the lower isotopic mass diffuse and react quicker and thus are utilized more frequently. This causes the strong ^{13}C depletion in microbial methane compared to the source material. The observed fractionation factor α for hydrogenotrophic methanogenesis varies

between 1.045 and 1.08, and between 1.00 and 1.032 for acetotrophic methanogeneis (Conrad, 2005 and references therein). Thus, microbial methane produced by the carbonate reduction pathway has more negative δ^{13}C values than methane produced by acetate fermentation (Figure 8).
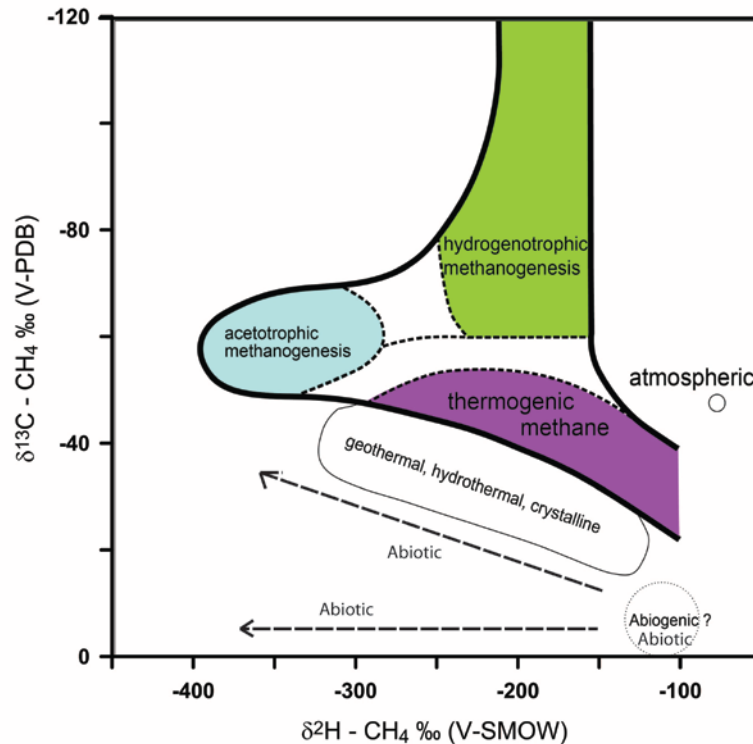
Figure 8: Schematic showing the different carbon and hydrogen isotope characteristics of microbial, thermogenic and abiotic methane (Whiticar, 1999; Etiope and Schoell, 2014). The dashed arrows originating in the abiotic methane field indicate recent findings of larger variation of abiotic methane isotope composition.

Thermogenic methane is generally enriched in ^{13}C compared to microbial methane. Several aspects can account for this ^{13}C enrichment: different precursor material (kerogen type), different kinetic isotope effect and higher temperature during thermogenic methane generation, which lowers the isotopic fractionation. The difference between δ^{13}C of the organic matter and methane roughly varies between 0‰ – 30‰ (Whiticar 1999). Assuming a δ^{13}C of organic matter of around -25‰ can result in thermogenic methane with an isotopic signature between -55‰ and -25‰ (Figure 8).

There is a slight overlap in δ^{13}C values of thermogenic methane and methane formed by acetotrophic methanogenesis between -50‰ and -60‰ (Figure 8). Including the information of the hydrogen isotopes of methane (δ^2H-CH$_4$), can help to differentiate between these two methane sources,

because the δ^2H values are considerably lighter for methane formed by microbial acetotrophic methanogenesis (Figure 8).

Until only a few years ago abiotic methane was believed to always be enriched in ^{13}C with δ^{13}C values above -25‰ (Figure 8), however recent studies have shown a wider range of carbon and hydrogen isotope composition of abiotic methane with δ^{13}C values as low as -37‰ for methane from serpentinized ultramafic rocks (Etiope and Schoell, 2014 and references therein).

4.5.2   Methane consumption

There is not only isotope fractionation occurring during methane formation, but also during methane consumption such as the aerobic and anaerobic oxidation of methane, which changes the δ^{13}C of the remaining methane. Estimates for the fractionation factor α during AOM based on pore water profiles vary between 1.009 and 1.024 (Whiticar and Faber, 1986; Alperin et al., 1988; Martens et al., 1999; Reeburgh et al., 2006). However, there is an overlap between the AOM horizon and the methanogenesis horizon in sediments, thus fractionation data from natural habitats are probably underestimates. (Holler et al., 2009) report fractionation factors of 1.012-1.039 determined using incubation experiments with ANME-2 methanotrophic archaea, where AOM was the only process. Hence, these are probably closer to the real α(AOM). For aerobic oxidation of methane a fractionation factor α of 1.027 was found based on incubation experiments (Kinnaman et al., 2007). In both cases of microbial consumption of methane (aerobic and anaerobic) the δ^{13}C of the remaining methane pool will increase during progressive consumption.

4.5.3   Petroleum biodegradation

Not only methane stable isotopes can help identify gas sources, also the isotope composition of other light hydrocarbons (ethane to butane), can shed light on processes of their formation or alteration. The most important alteration process of the carbon isotope composition of these hydrocarbons is through biodegradation, which takes place in petroleum reservoirs cooler than approximately 80°C. The degree of biodegradation generally increases towards cooler, shallower

reservoirs (Wenger et al., 2002). Continuing degradation of crude oil normally removes saturated hydrocarbons first, especially propane and *n*-butane are preferentially removed from natural gas (Wenger et al., 2002) (Table 2).

Table 2: Removal of selected compounds at various levels of biodegradation (from Wenger et al., 2002)

		Level of Biodegradation				
		very slight	slight	moderate	heavy	severe
C_1-C_5 gases	methane					
	ethane			▪▪▪▪		➜
	propane	▪▪▪▪▪▪▪▪▪▪				➜
	iso-butane			▪▪▪▪		➜
	n-butane		▪▪▪▪			➜
	pentanes		▪▪▪▪			➜

The general pattern of $\delta^{13}C$ of thermogenic C_1-C_4 hydrocarbons is enrichment in ^{13}C with increasing molecular mass (Figure 9). However, the preferential removal of certain compounds increases the $\delta^{13}C$ in the remaining fraction because breaking ^{12}C-^{12}C bonds requires less energy (Chung et al 1988), resulting in a changed $\delta^{13}C$ pattern. Thus propane normally shows strongest ^{13}C enrichment, because it is attacked first (Table 2), followed by *n*-butane (Figure 9).
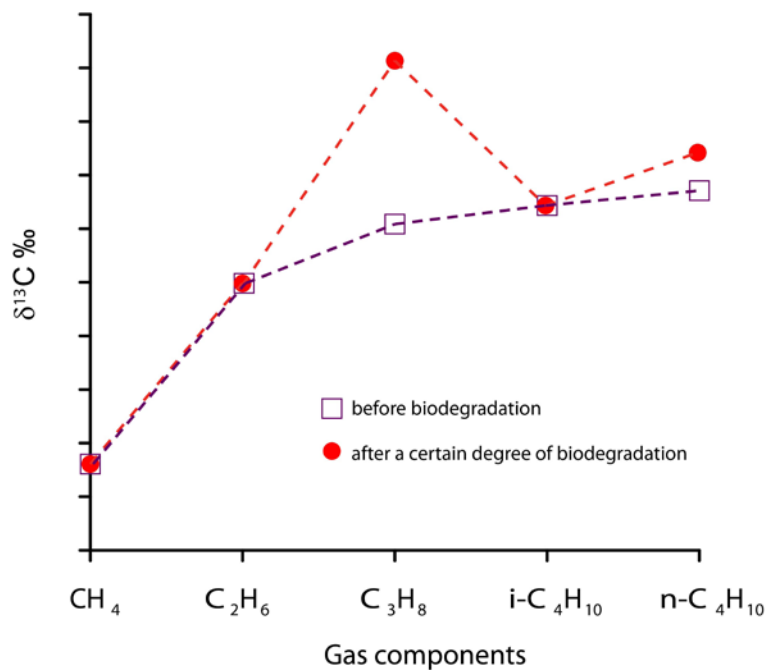

Figure 9: Schematic showing the $\delta^{13}C$ pattern on C1-C4 hydrocarbons before and after biodegradation.

Formerly, it was considered that petroleum biodegrading organisms require oxygen, however, more recently also anaerobic hydrocarbon degradation has been discovered, for example, mediated by sulphate-reducing bacteria (e.g. Jaekel et al., 2013). Most biodegrading organisms produce CO_2, which in turn can be the basis for secondary methanogenesis in anaerobic environments (Etiope et al., 2009).

4.6   Archives of methane seepage

Methane seepage can be recorded in authigenic carbonates as a result of high methane flux and high AOM rates causing increased carbonate alkalinity. Magnesium and calcium ions from the pore water together with bicarbonate are used to form these methane-derived authigenic carbonates (MDAC) (e.g. Ritger et al., 1987), also called cold seep carbonates. Depending on the Mg/Ca ratio in pore water, sulphate concentrations, phosphate concentrations, temperature, and probably other factors as well, different carbonate minerals form such as calcite, aragonite, Mg-calcite, protodolomite, dolomite and ankerite (Walter, 1986; Stakes et al., 1999; Moore et al., 2004). Both modern and ancient cold seep carbonates have been studied from various places around the globe (Table 3).

Table 3: Examples of studies of authigenic carbonates from low and mid latitude locations (left) and high latitude locations (right). Only in recent years have studies on authigenic carbonates on high latitude, formerly glaciated margins been published.

Authigenic carbonate studies from low and mid latitudes	Authigenic carbonate studies from high latitudes
•Gulf of mexico (Aharon et al., 1997; Bian et al., 2013; Feng et al., 2014) •Hydrate Ridge (Greinert et al., 2001; Teichert et al., 2003; Teichert et al., 2005) •Eastern mediterranean (Aloisi et al., 2000; Aloisi et al., 2002) •Black Sea (Mazzini et al., 2004; Bahr et al., 2009; Blumenberg et al., 2015) •Nile deep sea fan (Bayon et al., 2009; Gontharet et al., 2009; Römer et al., 2014) •Sea of marmara (Chevalier et al., 2011; Crémière et al., 2013) •Northern South China Sea (Lu et al., 2015; Guan et al., 2016)	•Bering sea (Pierre et al., 2014) •West Svalbard margin (Berndt et al., 2014) •Barents Sea (Crémière et al., 2016a) •Mid Norwegian margin (Hovland et al., 2005; Mazzini et al., 2006) •North Sea (Crémière et al., 2016b; Mazzini et al., 2016)

The involvement of AOM in the formation of seep carbonates was first shown by very low $\delta^{13}C$-carbonate values suggesting the main carbon source to be methane-carbon (e.g. Bohrmann et al., 1998). By now several studies investigating the biomarker content of seep carbonates have shown very low compound specific $\delta^{13}C$ values, as low as -140‰, of compounds believed to originate from microorganisms involved in AOM (Haas et al., 2010). Furthermore, microbiological studies show that seep carbonate are not only passive recorders of methane oxidation but represent a habitat for AOM microbial communities, too (Marlow et al., 2014).

A very important aspect of the study of seep carbonates is to determine the time of precipitation. Attempts of authigenic carbonate dating via radiocarbon dating have been made (e.g. Hiruta et al., 2014), however some of the carbon incorporated in the authigenic carbonates is "old carbon" derived from thermogenic methane which causes overestimation of the age, making the ^{14}C ages merely maximum age estimates. The best method for dating seep carbonates has been proven to be U-Th dating. U-Th dating (also referred to as ^{230}Th dating or ^{238}U-^{234}U-^{230}Th dating) of carbonates is based on the initial portion of the ^{238}U decay chain (Edwards et al., 2003). The relevant nuclides for carbonate dating are ^{238}U, ^{234}U, ^{230}Th, and ^{232}Th is typically measured as long-lived, basically stable index isotope. The time span covered by ^{230}Th dating is 3 to 600,000 years. The U-series dating method depends on the fractionation of the parent (^{238}U) and daughter (^{232}Th) nuclides by a natural process, and the knowledge of the initial amount of the daughter isotope. In carbonate dating the initial daughter concentration is in most cases negligible, because thorium has extremely low solubility in almost all waters, and is thus not incorporated into carbonate (Edwards et al., 2003). Carbonates take up uranium and thorium in almost the same proportion as in seawater, thus the initial $^{230}Th/^{238}U$ ratio in carbonates is extremely low, because thorium is insoluble in oxic waters whereas uranium is soluble in different forms.

Assuming an initial $^{230}Th/^{238}U = 0$, the ^{230}Th age equation is:

$$\left[\frac{^{230}\text{Th}}{^{238}\text{U}}\right] - 1 = -e^{-\lambda_{230}t} + \left(\frac{\delta^{234}\text{U}_m}{1000}\right)\left(\frac{\lambda_{230}}{\lambda_{230}-\lambda_{234}}\right)\left(1-e^{-(\lambda_{230}-\lambda_{234})t}\right)$$

where λ's are decay constants, [] indicate activity ratios, t is the age and $\delta^{234}\text{U}_m$ is the present deviation of $^{234}\text{U}/^{238}\text{U}$ from secular equilibrium. The initial $^{234}\text{U}/^{238}\text{U}$ ratio can be determined using the equation:

$$\delta^{234}\text{U}_m = \left(\delta^{234}\text{U}_i\right)e^{-\lambda_{234}t}$$

.

In marine samples the knowledge of $\delta^{234}\text{U}_i$ is important, because the marine $\delta^{234}\text{U}$ is assumed to have been constant. Hence, if the calculated $\delta^{234}\text{U}_i$ deviates too much from the marine $\delta^{234}\text{U}$, diagenetic shifts in uranium and potential inaccuracy in the ^{230}Th age could be the result (Edwards et al., 2003).

Another factor causing dating errors is the presence of detrital material in carbonates, because thorium is mostly adsorbed onto solid particles and thus initial $^{230}\text{Th}/^{238}\text{U}$ is not zero. This problem can, however, be solved by determining the $^{230}\text{Th}/^{232}\text{Th}$ of the sediments in the vicinity of the authigenic carbonates and using this initial [$^{230}\text{Th}/^{232}\text{Th}$] for correction.

5   Concluding remarks and outlook

This thesis represents an integrated research effort to understand past and present methane cycling on the northern Norwegian margin. Active hydrocarbon seeps in the Hola trough on the Vesterålen continental shelf are found to be fed predominantly by thermogenic methane (and ethane, propane and butane). Most likely derived from Late Jurassic to Early Cretaceous source rocks, these gaseous hydrocarbons migrate along major unconformities between the basement and the overlying Mesozoic sedimentary rocks. Most of the ascending methane is consumed by anaerobic oxidation of methane (AOM) at the sulphate methane transition (SMT) within the subsurface sediments. The SMT was identified at different depths in three gravity cores across the Hola trough, governed by different methane flux. Only in areas of focussed fluid flow, where gas flux exceeds the AOM capacity of the microbial communities in the sediment, methane enters the water column as gas bubbles. These gas escape sites are detected and mapped using a multibeam echosounder water column data set covering the study area, and are found to occur mainly in areas close to two cold water coral mounds not far from a regional fault crossing the Hola trough in a NE-SW direction (Figure 10).

Due to the very coarse grained surface sediments in the Hola trough, there is no pockmark formation induced by gas escape. However, further to the south several pockmark fields have been mapped (Figure 10) (mareano.no), which mostly lie along the same geological structure as the gas flares in the Hola trough, namely the Cretaceous Ribban basin. Pockmarks indicate that gas escape has taken place in these areas in the past, but whether gas is still actively seeping at these locations has to be proven. It is very likely that the same source rock responsible for the thermogenic methane generation in the Hola trough is also causing or has caused gas leakage at other places along this structure.
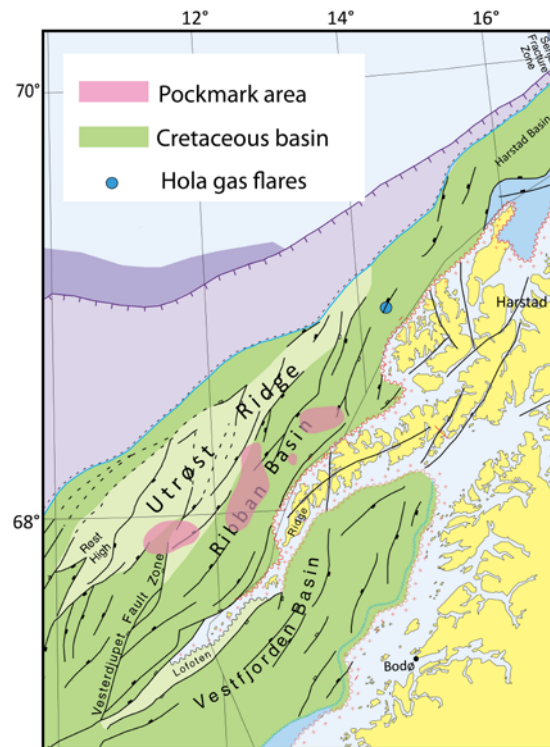
Figure 10: Relationship between the geological structure, the Cretaceous Ribban basin, and past and present methane seepage evidenced by pockmark areas (source:mareano.no) and gas flares.

The thermogenic origin of the gas was shown by the δ^{13}C values of methane, ethane, propane and butane. ^{13}C enrichment in propane and *n*-butane compared to the theoretical isotope trend of thermogenic gas further showed biodegradation of these compounds. This suggests that secondary methanogenesis, as a result of anaerobic petroleum biodegradation, may have caused the ^{13}C enriched dissolved inorganic carbon (DIC) below the SMT in Hola sediments. Such high δ^{13}C-DIC values, which are generally explained by hydrogenotrophic methanogenesis preferably removing ^{12}C from the DIC pool, are distinctly different from organic-rich sediments in Ullsfjorden, northern Norway. There, organic matter input and resulting methanogenesis rates are higher, however, δ^{13}C-DIC values below the SMT are significantly lower in the fjord sediments (-1.2‰) compared to the organic-poor Hola sediments (+19‰). This corroborates the idea that isotopically heavy DIC in Hola is supplied to the system by ascending fluids influenced by anaerobic petroleum degradation and secondary methanogenesis. To investigate this interpretation further, a longer sediment core from the Hola area would be beneficial to understand how the δ^{13}C-DIC pattern continues below 3 m

sediment depths (maximum depth of our gravity cores from the study area). Moreover, for future investigations of the Hola seep area the aim should be to obtain sediment cores with video guidance. In this way, samples directly at or adjacent to gas escape sites could be chosen and investigated where the SMT is suspected to be just a few centimetres or tens of centimetres below the sediment surface, and the sulphate pore water profile is expected to show signs of fluid advection (non-linear profiles). Another goal should be to obtain gas samples of the gas escaping to the water column. Compositional and isotopic changes of this gas, compared to the gas we analysed in the sediment would provide further insight into processes at the interface between the sediment and the water column. Furthermore, the 'Lofoten-Vesterålen Cabled Ocean Observatory' (LoVe) (http://love.statoil.com/), initiated by the Institute of Marine Research (IMR) and Statoil, was installed in the Hola trough in 2013 and is supposed to get extended by several stations in the coming years, one of which will be placed at our investigated seep site. This observatory is planned to host several sensors for long term monitoring of the seep site to improve the understanding of the dynamics of these seeps.

In our comparison study between Hola and Ullsfjorden we showed that although the sulphate profiles in these two cores are very similar (linear profiles and SO_4 depletion between 100 and 150 cm), the environments and prevailing processes are very different. The organic carbon source in the fjord is almost exclusively labile marine organic matter, which is the basis for high rates of organoclastic sulphate reduction, releasing ammonium and phosphate to the pore water as reflected in the pore water profiles. Less than half of the depth-integrated sulphate reduction in this core is coupled to AOM, indicating that in the fjord setting the SMT depth is influenced more by organic matter deposition and degradation than by methane ascent. The situation in Hola sediments is the opposite. Organic matter composition shows a stronger terrestrial influence and overall concentrations are lower due to dominantly coarser grained sediments. Nevertheless, sulphate is depleted at an even shallower depth than in the fjord sediments. This indicates that the SMT depth in Hola is controlled mainly by methane ascent, which is supported by modelling results showing that

96% of depth-integrated sulphate reduction is coupled to AOM. Multiple times lower ammonium concentrations in Hola sediments than in the fjord sediments support this inference, because AOM does not produce ammonium whereas organoclastic sulphate reduction does. An important finding from this study is that no conclusions about prevailing processes can be drawn from sulphate pore water profiles alone, but other factors such as sedimentary organic carbon content and burial, pore water ammonium and phosphate, and δ^{13}C of DIC and methane have to be considered as well.

We could furthermore show that in fjord sediments where methane carbon and hydrogen isotopes clearly prove a microbial methane origin, we can still find higher hydrocarbons such as ethane and propane. Additionally, the carbon isotope composition of ethane and propane is considerably lighter than in thermogenically produced C2 and C3 hydrocarbons, consistent with a microbial origin. Microbial formation of ethane and propane has been proposed previously but an exact process of their formation is not known yet.

The study of methane-derived authigenic carbonates in the Hola trough revealed two different mineralogical types. We interpreted aragonite-dominated carbonates to have formed closer to the sediment surface under conditions of higher AOM rates and thus stronger methane flux and also stronger seawater influence. On the other hand, dolomite-dominated nodules appear to have formed deeper within the sediment under more restricted conditions and lower methane fluxes. However, we cannot define a certain sediment depth where aragonite precipitation has been replaced by dolomite precipitation. At the present depth of the SMT in core GC 51 dolomite precipitation is likely occurring because there is a slight indication in the solid phase chemistry (Ca/Ti peak) of carbonate precipitation. Furthermore, Ca^{2+} and Mg^{2+} pore water diffusion calculations indicate similar diffusion rates of these two constituents between the bottom water and the SMT (Appendix). A core adjacent to a gas escape site with a SMT very close the seafloor (as suggested above) could help reveal at which depth dolomite precipitation is still the dominant process or aragonite precipitation could be occurring. Hence, further studies of well placed sediment cores from

Hola may allow establishing the mineralogical approach for defining the depth of SMT and methane flux rates.

Three intervals containing dolomite nodules were identified in gravity core GC 51, indicating recurring changes in methane flux followed by times of stable methane flux allowing nodule formation at the SMT. In all nodules authigenic barite minerals were observed under the scanning electron microscope, which typically form at the SMT from downward diffusing sulphate and upward diffusing barium. Determining the amount of authigenic barite formed in each interval could help constrain the time periods necessary to form the observed dolomite nodules in the different depths and provide further information on methane flux dynamics at a single location. Furthermore, multiple sulphur isotope studies of barite and co-existing pyrite and carbonate associated sulphate may shed light on the process of dissimalatory sulphur metabolism of AOM.

The most important information derived from the MDAC's are the temporal constraints of methane escape inferred from U-Th dating. Based on our present knowledge, methane seepage in the Hola trough started at least 11 ka ago, probably even slightly before (the earliest carbonate cement formation could not be dated). It seems likely that strongest events of past methane seepage and carbonate formation occurred around 10, 4 and 2 ka BP. The events may be tentatively correlated to seismicity events related to isostatic rebound of the lithospheric crust after retreat and melting of the Scandinavian ice sheet and local/regional earthquakes, which are known to enable fluid flow due to pore pressure changes or reactivation of faults. However, the present data coverage of U-Th dated MDAC is not sufficient to draw solid conclusions. More systematic sampling of MDAC crusts will be required for the future and the combination of data collect by the LoVe observatory mentioned above. It is anticipated that the observatory will record both methane seepage and seismicity in the future (camera, methane sensors, ocean bottom seismometer) to improve the understanding of which factors control methane seepage in the Hola trough. The suggested link between seismicity

and methane escape can be tested, and moreover, a possible strengthening or weakening of methane escape in the future could be monitored.

6 References

Albretsen, J., Sperrevik, A.K., Staalstrøm, A., Sandvik, A.D., Vikebø, F., Asplin, L., 2011. NorKyst-800 Report No. 1 - User Manual and technical descriptions, Fisken og Havet. Institute of Marine Research.

Alperin, M.J., Reeburgh, W.S., Whiticar, M.J., 1988. Carbon and hydrogen isotope fractionation resulting from anaerobic methane oxidation. Journal Name: Global Biogeochemical Cycles; (USA); Journal Volume: 2:3: Medium: X; Size: Pages: 279-288.

Badr, O., Probert, S.D., O'Callaghan, P.W., 1991. Atmospheric methane: Its contribution to global warming. Applied Energy, 40(4): 273-313.

Batchelor, C.L., Dowdeswell, J.A., 2015. Ice-sheet grounding-zone wedges (GZWs) on high-latitude continental margins. Marine Geology, 363: 65-92.

Beal, E.J., House, C.H., Orphan, V.J., 2009. Manganese- and Iron-Dependent Marine Methane Oxidation. Science, 325(5937): 184-187.

Bekryaev, R.V., Polyakov, I.V., Alexeev, V.A., 2010. Role of Polar Amplification in Long-Term Surface Air Temperature Variations and Modern Arctic Warming. Journal of Climate, 23(14): 3888-3906.

Bellec, V., Bøe, R., Thorsnes, T., Rise, L., Dolan, M., Elvenes, S., Lepland, A., Selboskar, O.H., 2012. Geologisk Havbunnskart, Kart 6183001400. Norges geologiske undersøkelse.

Bergh, S.G., Eig, K., Kløvjan, O.S., Henningsen, T., Olesen, O., Hansen, J.A., 2007. The Lofoten-Vesterålen continental margin: a multiphase Mesozoic-Palaeogene rifted shelf as shown by offshore-onshore brittle fault-fracture analysis. Norwegian Journal of Geology, 87: 29-58.

Blystad, P., Brekke, H., Færseth, R.B., Larsen, B.T., Skogseid, J., Tørudbakken, B., 1995. Structural Elements of the Norwegian Continental Shelf. Norwegian Petroleum Directorate - Bulletin 8.

Boetius, A., Ravenschlag, K., Schubert, C.J., Rickert, D., Widdel, F., Gieseke, A., Amann, R., Jorgensen, B.B., Witte, U., Pfannkuche, O., 2000. A marine microbial consortium apparently mediating anaerobic oxidation of methane. Nature, 407(6804): 623-626.

Bohrmann, G., Greinert, J., Suess, E., Torres, M., 1998. Authigenic carbonates from the Cascadia subduction zone and their relation to gas hydrate stability. Geology, 26(7): 647-650.

Boudreau, B., 1997. Diagenetic models and their impletation: modelling transport and reactions in aquatic sediments. Springer, Berlin, Heidelberg, NY, 414 pp.

Byrkjeland, U., Bungum, H., Eldholm, O., 2000. Seismotectonics of the Norwegian continental margin. Journal of Geophysical Research: Solid Earth, 105(B3): 6221-6236.

Bøe, R., Bellec, V.K., Dolan, M.F.J., Buhl-Mortensen, P., Buhl-Mortensen, L., Slagstad, D., Rise, L., 2009. Giant sandwaves in the Hola glacial trough off Vesterålen, North Norway. Marine Geology, 267(1–2): 36-54.

Cannat, M., Fontaine, F., Escartín, J., 2010. Serpentinization and Associated Hydrogen And Methane Fluxes at Slow Spreading Ridges, Diversity Of Hydrothermal Systems On Slow Spreading Ocean Ridges. American Geophysical Union, pp. 241-264.

Chand, S., Rise, L., Bellec, V., Dolan, M., Bøe, R., Thorsnes, T., Buhl-Mortensen, P., 2008. Active Venting System Offshore Northern Norway. Eos, Transactions American Geophysical Union, 89(29): 261-262.

Change), I.I.P.o.C., 2001. Climate Change 2001 - The Scientific Basis, Cambridge University Press, Cambridge UK, 881 pp.

Clayton, C., 1991. Carbon isotope fractionation during natural gas generation from kerogen. Marine and Petroleum Geology, 8(2): 232-240.

Conrad, R., 2005. Quantification of methanogenic pathways using stable carbon isotopic signatures: a review and a proposal. Organic Geochemistry, 36(5): 739-752.

D'Hondt, S., Rutherford, S., Spivack, A.J., 2002. Metabolic Activity of Subsurface Life in Deep-Sea Sediments. Science, 295(5562): 2067-2070.

Dickens, G.R., 2011. Down the Rabbit Hole: toward appropriate discussion of methane release from gas hydrate systems during the Paleocene-Eocene thermal maximum and other past hyperthermal events. Clim. Past, 7(3): 831-846.

Dlugokencky, E.J., Nisbet, E.G., Fisher, R., Lowry, D., 2011. Global atmospheric methane: budget, changes and dangers. Philosophical Transactions of the Royal Society A: Mathematical, Physical and Engineering Sciences, 369(1943): 2058-2072.

Dowdeswell, J.A., Kenyon, N.H., Elverhøi, A., Laberg, J.S., Hollender, F.J., Mienert, J., Siegert, M.J., 1996. Large-scale sedimentation on the glacier-influenced polar North Atlantic Margins: Long-range side-scan sonar evidence. Geophysical Research Letters, 23(24): 3535-3538.

Edwards, R.L., Gallup, C.D., Cheng, H., 2003. Uranium-series Dating of Marine and Lacustrine Carbonates. Reviews in Mineralogy and Geochemistry, 52(1): 363-405.

Eidvin, T., Riis, F., Rasmussen, E.S., 2014. Oligocene to Lower Pliocene deposits of the Norwegian continental shelf, Norwegian Sea, Svalbard, Denmark and their relation to the uplift of Fennoscandia: A synthesis. Marine and Petroleum Geology, 56: 184-221.

Etheridge, D.M., Steele, L.P., Francey, R.J., Langenfelds, R.L., 1998. Atmospheric methane between 1000 A.D. and present: Evidence of anthropogenic emissions and climatic variability. Journal of Geophysical Research: Atmospheres, 103(D13): 15979-15993.

Etiope, G., Feyzullayev, A., Milkov, A.V., Waseda, A., Mizobe, K., Sun, C.H., 2009. Evidence of subsurface anaerobic biodegradation of hydrocarbons and potential secondary methanogenesis in terrestrial mud volcanoes. Marine and Petroleum Geology, 26(9): 1692-1703.

Etiope, G., Sherwood Lollar, B., 2013. Abiotic methane on Earth. Reviews of Geophysics, 51(2): 276-299.

Etiope, G., Schoell, M., 2014. Abiotic Gas: Atypical, But Not Rare. Elements, 10(4): 291-296.

Ettwig, K.F., Shima, S., Van De Pas-Schoonen, K.T., Kahnt, J., Medema, M.H., Op Den Camp, H.J.M., Jetten, M.S.M., Strous, M., 2008. Denitrifying bacteria anaerobically oxidize methane in the absence of Archaea. Environmental Microbiology, 10(11): 3164-3173.

Faleide, J.I., Tsikalas, F., Breivik, A.J., Mjelde, R., Ritzmann, O., Engen, Ø., Wilson, J., Eldholm, O., 2008. Structure and evolution of the continental margin off Norway and the Barents Sea. Episodes, 31(1): 82-91.

Fischer, D., Sahling, H., Nöthen, K., Bohrmann, G., Zabel, M., Kasten, S., 2012. Interaction between hydrocarbon seepage, chemosynthetic communities, and bottom water redox at cold seeps of the Makran accretionary prism: insights from habitat-specific pore water sampling and modeling. Biogeosciences, 9(6): 2013-2031.

Floodgate, G.D., Judd, A.G., 1992. Methane in Marine SedimentsThe origins of shallow gas. Continental Shelf Research, 12(10): 1145-1156.

Froelich, P.N., Klinkhammer, G.P., Bender, M.L., Luedtke, N.A., Heath, G.R., Cullen, D., Dauphin, P., Hammond, D., Hartman, B., Maynard, V., 1979. Early oxidation of organic matter in pelagic sediments of the eastern equatorial Atlantic: suboxic diagenesis. Geochimica et Cosmochimica Acta, 43(7): 1075-1090.

Glasby, G.P., 2006. Abiogenic Origin of Hydrocarbons: An Historical Overview. Resource Geology, 56(1): 83-96.

Godø, O.R., Tenningen, E., Ostrowski, M., Kubilius, R., Kutti, T., Korneliussen, R., Fosså, J.H., 2012. The Hermes Lander project – the technology, the data and evaluation of concept and results, Institute of Marine Research (Havforskningsinstituttet).

Haas, A., Peckmann, J., Elvert, M., Sahling, H., Bohrmann, G., 2010. Patterns of carbonate authigenesis at the Kouilou pockmarks on the Congo deep-sea fan. Marine Geology, 268(1–4): 129-136.

Haflidason, H., Lien, R., Petter Sejrup, H., Forsberg, C.F., Bryn, P., 2005. The dating and morphometry of the Storegga Slide, Ormen Lange–an Integrated Study for Safe Field Development in the Storegga Submarine Area. Elsevier, Oxford, pp. 123-136.

Henningsen, T., Tveten, E., 1998. Berggrunnskart ANDØYA, M 1:250 000. Norges Geologiske Undersøkelse, Trondheim.

Hinrichs, K.-U., Hayes, J.M., Sylva, S.P., Brewer, P.G., DeLong, E.F., 1999. Methane-consuming archaebacteria in marine sediments. Nature, 398(6730): 802-805.

Hinrichs, K.-U., Boetius, A., 2003. The Anaerobic Oxidation of Methane: New Insights in Microbial Ecology and Biogeochemistry. In: Wefer, G. et al. (Eds.), Ocean Margin Systems. Springer Berlin Heidelberg, Berlin, Heidelberg, pp. 457-477.

Hiruta, A., Wang, L.-C., Ishizaki, O., Matsumoto, R., 2014. Last glacial emplacement of methane-derived authigenic carbonates in the Sea of Japan constrained by diatom assemblage, carbon-14, and carbonate content. Marine and Petroleum Geology, 56: 51-62.

Holler, T., Wegener, G., Knittel, K., Boetius, A., Brunner, B., Kuypers, M.M.M., Widdel, F., 2009. Substantial 13C/12C and D/H fractionation during anaerobic oxidation of methane by marine consortia enriched in vitro. Environmental Microbiology Reports, 1(5): 370-376.

Hovland, M., Judd, A.G., 1988. Seabed Pockmarks and Seepages. Impact on Geology, Biology and Marine Environment. Graham & Trotman London, Dordrecht, Boston, 293 pp.

Jaekel, U., Musat, N., Adam, B., Kuypers, M., Grundmann, O., Musat, F., 2013. Anaerobic degradation of propane and butane by sulfate-reducing bacteria enriched from marine hydrocarbon cold seeps. ISME J, 7(5): 885-895.

Johnson, J.E., Mienert, J., Plaza-Faverola, A., Vadakkepuliyambatta, S., Knies, J., Bünz, S., Andreassen, K., Ferré, B., 2015. Abiotic methane from ultraslow-spreading ridges can charge Arctic gas hydrates. Geology.

Judd, A., 2004. Natural seabed gas seeps as sources of atmospheric methane. Environmental Geology, 46(8): 988-996.

Judd, A.G., 2000. Geological Sources of Methane. In: Khalil, M. (Ed.), Atmospheric Methane. Springer Berlin Heidelberg, pp. 280-303.

Judd, A.G., Hovland, M., 2007. Seabed fluid flow. Cambridge University Press, New York.

Kennett, J.P., Cannariato, K.G., Hendy, I.L., Behl, R.J., 2000. Carbon Isotopic Evidence for Methane Hydrate Instability During Quaternary Interstadials. Science, 288(5463): 128-133.

Kinnaman, F.S., Valentine, D.L., Tyler, S.C., 2007. Carbon and hydrogen isotope fractionation associated with the aerobic microbial oxidation of methane, ethane, propane and butane. Geochimica et Cosmochimica Acta, 71(2): 271-283.

Kirschke, S., Bousquet, P., Ciais, P., Saunois, M., Canadell, J.G., Dlugokencky, E.J., Bergamaschi, P., Bergmann, D., Blake, D.R., Bruhwiler, L., Cameron-Smith, P., Castaldi, S., Chevallier, F., Feng, L., Fraser, A., Heimann, M., Hodson, E.L., Houweling, S., Josse, B., Fraser, P.J., Krummel, P.B., Lamarque, J.-F., Langenfelds, R.L., Le Quere, C., Naik, V., O'Doherty, S., Palmer, P.I., Pison, I., Plummer, D., Poulter, B., Prinn, R.G., Rigby, M., Ringeval, B., Santini, M., Schmidt, M., Shindell, D.T., Simpson, I.J., Spahni, R., Steele, L.P., Strode, S.A., Sudo, K., Szopa, S., van der Werf, G.R., Voulgarakis, A., van Weele, M., Weiss, R.F., Williams, J.E., Zeng, G., 2013. Three decades of global methane sources and sinks. Nature Geosci, 6(10): 813-823.

Kvenvolden, K.A., Rogers, B.W., 2005. Gaia's breath—global methane exhalations. Marine and Petroleum Geology, 22(4): 579-590.

Laberg, J.S., Vorren, T.O., 2000. The Trænadjupet Slide, offshore Norway — morphology, evacuation and triggering mechanisms. Marine Geology, 171(1–4): 95-114.

Laberg, J.S., Vorren, T.O., Dowdeswell, J.A., Kenyon, N.H., Taylor, J., 2000. The Andøya Slide and the Andøya Canyon, north-eastern Norwegian–Greenland Sea. Marine Geology, 162(2–4): 259-275.

Laberg, J.S., Stoker, M.S., Dahlgren, K.I.T., Haas, H.d., Haflidason, H., Hjelstuen, B.O., Nielsen, T., Shannon, P.M., Vorren, T.O., van Weering, T.C.E., Ceramicola, S., 2005. Cenozoic alongslope processes and sedimentation on the NW European Atlantic margin. Marine and Petroleum Geology, 22(9–10): 1069-1088.

Lashof, D.A., Ahuja, D.R., 1990. Relative contributions of greenhouse gas emissions to global warming. Nature, 344(6266): 529-531.

Lee, S.-Y., Holder, G.D., 2001. Methane hydrates potential as a future energy source. Fuel Processing Technology, 71(1–3): 181-186.

Lelieveld, J.O.S., Crutzen, P.J., Dentener, F.J., 1998. Changing concentration, lifetime and climate forcing of atmospheric methane. Tellus B, 50(2): 128-150.

Makogon, Y.F., Holditch, S.A., Makogon, T.Y., 2007. Natural gas-hydrates — A potential energy source for the 21st Century. Journal of Petroleum Science and Engineering, 56(1–3): 14-31.

Marlow, J.J., Steele, J.A., Ziebis, W., Thurber, A.R., Levin, L.A., Orphan, V.J., 2014. Carbonate-hosted methanotrophy represents an unrecognized methane sink in the deep sea. Nat Commun, 5.

Martens, C.S., Albert, D.B., Alperin, M.J., 1999. Stable isotope tracing of anaerobic methane oxidation in the gassy sediments of Eckernfoerde Bay, German Baltic Sea. American Journal of Science, 299(7-9): 589-610.

McGinnis, D.F., Greinert, J., Artemov, Y., Beaubien, S.E., Wüest, A., 2006. Fate of rising methane bubbles in stratified waters: How much methane reaches the atmosphere? Journal of Geophysical Research: Oceans, 111(C9): C09007.

Moore, T.S., Murray, R.W., Kurtz, A.C., Schrag, D.P., 2004. Anaerobic methane oxidation and the formation of dolomite. Earth and Planetary Science Letters, 229(1–2): 141-154.

Orphan, V.J., House, C.H., Hinrichs, K.-U., McKeegan, K.D., DeLong, E.F., 2001. Methane-Consuming Archaea Revealed by Directly Coupled Isotopic and Phylogenetic Analysis. Science, 293(5529): 484-487.

Ottesen, D., Dowdeswell, J.A., Rise, L., Rokoengen, K., Henriksen, S., 2002. Large-scale morphological evidence for past ice-stream flow on the mid-Norwegian continental margin. Geological Society, London, Special Publications, 203(1): 245-258.

Plassen, L., Vorren, T.O., 2003a. Sedimentary processes and the environment during deglaciation of a fjord basin in Ullsfjorden, North Norway. Norwegian Journal of Geology, 83: 23-26.

Plassen, L., Vorren, T.O., 2003b. Fluid flow features in fjord-fill deposits, Ullsfjorden, North Norway. Norwegian Journal of Geology, 83: 37-42.

Raghoebarsing, A.A., Pol, A., van de Pas-Schoonen, K.T., Smolders, A.J.P., Ettwig, K.F., Rijpstra, W.I.C., Schouten, S., Damste, J.S.S., Op den Camp, H.J.M., Jetten, M.S.M., Strous, M., 2006. A microbial consortium couples anaerobic methane oxidation to denitrification. Nature, 440(7086): 918-921.

Reeburgh, W.S., 1976. Methane consumption in Cariaco Trench waters and sediments. Earth and Planetary Science Letters, 28(3): 337-344.

Reeburgh, W.S., Tyler, S.C., Carroll, J., 2006. Stable carbon and hydrogen isotope measurements on Black Sea water-column methane. Deep Sea Research Part II: Topical Studies in Oceanography, 53(17–19): 1893-1900.

Reeburgh, W.S., 2007. Oceanic Methane Biogeochemistry. Chemical Reviews, 107(2): 486-513.

Rice, D.D., 1992. Controls, habitat, and resource potential of ancient bacterial gas. In: Vially, R. (Ed.), Bacterial Gas. Editions Technip, Paris, pp. 91-118.

Ritger, S., Carson, B., Suess, E., 1987. Methane-derived authigenic carbonates formed by subduction-induced pore-water expulsion along the Oregon/Washington margin. Geological Society of America Bulletin, 98(2): 147-156.

Rooze, J., Egger, M., Tsandev, I., Slomp, C.P., 2016. Iron-dependent anaerobic oxidation of methane in coastal surface sediments: Potential controls and impact. Limnology and Oceanography: n/a-n/a.

Rydningen, T.A., Laberg, J.S., Kolstad, V., 2015. Late Cenozoic evolution of high-gradient trough mouth fans and canyons on the glaciated continental margin offshore Troms, northern Norway—Paleoclimatic implications and sediment yield. Geological Society of America Bulletin.

Rørvik, K.L., Laberg, J.S., Hald, M., Ravna, E.K., Vorren, T.O., 2010. Behavior of the northwestern part of the Fennoscandian Ice Sheet during the Last Glacial Maximum – a response to external forcing. Quaternary Science Reviews, 29(17–18): 2224-2237.

Schulz, H.D., 2006. Quantification of Early Diagenesis: Dissolved Constituents in Pore Water and Signals in the Solid Phase. In: Schulz, H.D., Zabel, M. (Eds.), Marine Geochemistry. Springer Berlin Heidelberg, pp. 73-124.

Scranton, M.I., Brewer, P.G., 1978. Consumption of dissolved methane in the deep ocean. Limnology and Oceanography, 23(6).

Shakhova, N., Semiletov, I., Salyuk, A., Yusupov, V., Kosmach, D., Gustafsson, Ö., 2010. Extensive Methane Venting to the Atmosphere from Sediments of the East Siberian Arctic Shelf. Science, 327(5970): 1246-1250.

Sommer, S., Pfannkuche, O., Linke, P., Luff, R., Greinert, J., Drews, M., Gubsch, S., Pieper, M., Poser, M., Viergutz, T., 2006. Efficiency of the benthic filter: Biological control of the emission of dissolved methane from sediments containing shallow gas hydrates at Hydrate Ridge. Global Biogeochemical Cycles, 20(2): n/a-n/a.

Stakes, D.S., Orange, D., Paduan, J.B., Salamy, K.A., Maher, N., 1999. Cold-seeps and authigenic carbonate formation in Monterey Bay, California. Marine Geology, 159(1–4): 93-109.

Steinle, L., Graves, C.A., Treude, T., Ferre, B., Biastoch, A., Bussmann, I., Berndt, C., Krastel, S., James, R.H., Behrens, E., Boning, C.W., Greinert, J., Sapart, C.-J., Scheinert, M., Sommer, S., Lehmann, M.F., Niemann, H., 2015. Water column methanotrophy controlled by a rapid oceanographic switch. Nature Geosci, 8(5): 378-382.

Thorsnes, T., Bøe, R., Bellec, V., Dolan, M., Rise, L., Elvenes, S., Ottesen, D., 2015. Chapter 4: The shelf off Lofoten, Vesterålen and Troms. In: Buhl-Mortensen, L., Hodnesdal, H., Thorsnes, T. (Eds.), The Norwegian Seafloor - New Knowledge from MAREANO for Ecosystem-Based Management.

Tsikalas, F., Eldholm, O., Faleide, J.I., 2005. Crustal structure of the Lofoten–Vesterålen continental margin, off Norway. Tectonophysics, 404(3–4): 151-174.

Valentine, D.L., 2002. Biogeochemistry and microbial ecology of methane oxidation in anoxic environments: a review. Antonie van Leeuwenhoek, 81(1): 271-282.

Vorren, T.O., Hald, M., Thomsen, E., 1984. Quaternary sediments and environments on the continental shelf off northern Norway. Marine Geology, 57(1–4): 229-257.

Vorren, T.O., Lebesbye, E., Andreassen, K., Larsen, K.B., 1989. Glacigenic sediments on a passive continental margin as exemplified by the Barents Sea. Marine Geology, 85(2–4): 251-272.

Vorren, T.O., Rydningen, T.A., Baeten, N.J., Laberg, J.S., 2015. Chronology and extent of the Lofoten–Vesterålen sector of the Scandinavian Ice Sheet from 26 to 16 cal. ka BP. Boreas: Advance online publication.

Walter, L.M., 1986. Relative efficiency of carbonate dissolution and precipitation during diagenesis: A progress report on the role of solution chemistry. In: Gautier, G.L. (Ed.), Roles of Organic Matter in Mineral Diagenesis. Society of Economic Palaeontologists and Mineralogists, Special Publications, pp. 1-12.

Wenger, L.M., Davis, C.L., Isaksen, G.H., 2002. Multiple controls on petroleum biodegradation and impact in oil quality. SPE Reservoir Eval. Engin., 5: 375-383.

Whiticar, M.J., Faber, E., 1986. Methane oxidation in sediment and water column environments—Isotope evidence. Organic Geochemistry, 10(4): 759-768.

Whiticar, M.J., 1999. Carbon and hydrogen isotope systematics of bacterial formation and oxidation of methane. Chemical Geology, 161(1–3): 291-314.

Whiticar, M.J., 2000. Can Stable Isotopes and Global Budgets Be Used to Constrain Atmospheric Methane Budgets? In: Khalil, M. (Ed.), Atmospheric Methane. Springer Berlin Heidelberg, pp. 63-85.

7 Appendix

To asses diffusive fluxes of dissolved pore water constituents in the different gravity cores we used Fick's first law of diffusion:

$$J_{sed} = -\Phi * D_{sed} * \frac{\partial C}{\partial x}$$

with J_{sed} being the diffusive flux in the sediment $[\text{mol m}^{-2}\text{s}^{-1}]$ and $\frac{\partial C}{\partial x}$ the concentration gradient $[mol/m^3 m]$ which was estimated based on the pore water concentration profiles (Schulz, 2006). The bulk sediment diffusion coefficient $D_{sed}[\text{m}^2\text{s}^{-1}]$ was determined by dividing the diffusion coefficient in seawater $D_{sw}[\text{m}^2\text{s}^{-1}]$ (Boudreau, 1997) by the tortuosity θ^2 to take into account that the ions cannot diffuse in a straight course in the sediment $(D_{sed} = \frac{D_{sw}}{\theta^2})$. The tortuosity was estimated based on the porosity ϕ and the relationship $\theta^2 = 1 - ln(\Phi^2)$ (Boudreau, 1997).

The results are summarized in Table 1

Table 4: Input parameters and results of 1D diffusion calculations using Fick's first law of diffusion. A porosity of 0.8 and resulting tortuosity of 1.45 was used for all the calculations

core	ion	diffusion coefficient in seawater [m²/s] for 5°C	diffusion coefficient in sediments [m²/s]	dC/dx [mol/m³m]	diffusive flux [mmol/m²a]
GC-51	SO_4^{2-}			32.7	J_{SO4} down = 325.4
GC-51	HS^-	1.11E-09	7.66E-10	-10.7	J_{HS-} up = 206.7
				5.9	J_{HS-} down = 113.8
GC-51	Ca^{2+}	4.26E-10	2.94E-10	-8.2	J_{Ca} down = 61.1
				0.8	J_{Ca} up = 5.98
GC-51	Mg^{2+}	3.93E-10	2,71E-10	-7.85	J_{Ca} down = 54

References

Boudreau, B., 1997. Diagenetic models and their impletation: modelling transport and reactions in aquatic sediments. Springer, Berlin, Heidelberg, NY, 414 pp.

Schulz, H.D., 2006. Quantification of Early Diagenesis: Dissolved Constituents in Pore Water and Signals in the Solid Phase. In: Schulz, H.D., Zabel, M. (Eds.), Marine Geochemistry. Springer Berlin Heidelberg, pp. 73-124.